Asian Journal of Geological Research

3(2): 17-33, 2020; Article no.AJOGER.57292

Structural Analysis Using Integrated Aeromagnetic Data and Landsat Imagery in a Basement Complex Terrain, Southwestern Nigeria

S. O. Ilugbo[1*], H. O. Edunjobi[2], O. E. Adewoye[3], T. O. Alabi[4], A. I. Aladeboyeje[3], O. O. Olutomilola[5] and D. T. Owolabi[6]

[1]Department of Applied Geophysics, Federal University of Technology, Akure, Ondo State, Nigeria.
[2]Department of Physics, Federal University of Agriculture Abeokuta, Abeokuta, Nigeria.
[3]Department of Physical Sciences, Ondo State University of Science and Technology, Okitipupa, Ondo State, Nigeria.
[4]Southwest Drilling, Borehole House Km 14 Ojoo-Iwo Road Express Way Ibadan, Oyo State, Nigeria.
[4]Dextol Global Geophysics, Km 14 Ojoo-Iwo Road Express Way Ibadan, Oyo State, Nigeria.
[5]Department of Geology, Afe Babalola University, Ado Ekiti, Nigeria.
[6]Department of Pure and Applied Physics, Ladoke Akintola University of Technology, Ogbomoso, Nigeria.

Authors' contributions

This work was carried out in collaboration among all authors. Author SOI designed the study, performed the statistical analysis, wrote the protocol and wrote the first draft of the manuscript. Authors HOE, OEA, TOA and AIA managed the analyses of the study. Authors OOO and DTO managed the literature searches. All authors read and approved the final manuscript.

Article Information

Editor(s):
(1) Dr. Ahmed Abdelraheem Frghaly, Sohag University, Egypt.
Reviewers:
(1) Lauro Cézar Montefalco de Lira Santos, Federal University of Pernambuco, Brazil.
(2) Klemen Zakšek, Germany.
Complete Peer review History: http://www.sdiarticle4.com/review-history/57292

Original Research Article

Received 10 March 2020
Accepted 16 May 2020
Published 26 May 2020

ABSTRACT

In this study, different digital format data sources including aeromagnetic and remotely sensed (Landsat ETM+) data were used for structural and tectonic interpretation of the southwestern part of Ilesha, Osun State, Nigeria. Aeromagnetic data were analyzed using advanced processing techniques (Spectral analysis, deconvolution). The aeromagnetic interpretation was carried out using the Butterworth filter, reduction to equator, derivative filters and Euler deconvolution. The results were improved by the study of enhanced Landsat ETM+ images and correlated with the

**Corresponding author: Email: bussytex4peace44@gmail.com;*

extracted surface lineaments. Two main lineament sets are observed in the study area. The major lineaments strike NW-SE, NE-SW and the minor E-W. General coincidence of both landsat and aeromagnetic lineaments trends were observed in the study area, reflecting the real continuous fractures in the depth. The 3D Euler deconvolution and radial spectral analysis applied to locate and estimate the depth to anomalous bodies, shows varying depth between 48 m and 280 m. The map revealed the presence of major and minor faults, fractures as well as rock boundaries with the frequency of fracturing. This suggests that the major fractures and faults in the area are deep seated within the basement formation since that the spectral analysis enhances the anomalies associated with deep magnetic sources. The processed image displays the lineaments trending NE-SW directions. The new structural map derived from the combined aeromagnetic data and landsat imagery, provides an effective tool for analyzing subsurface structure in the region.

Keywords: Aeromagnetic data; lands at Imagery; structural lineament; euler deconvolution; magnetic structures; depth-to-magnetic source.

1. INTRODUCTION

Magnetometry method is one of the best geoghysical techniques to delineate subsurface structures. Generally, aeromagnetic maps reflect the variations in the magnetic field of the earth. Based on the fact that magnetic observations are obtained relatively easily and cheaply and few corrections must be applied to the observations. Despite these obvious advantages, like the gravitational methods, interpretations of magnetic observations suffer from a lack of uniqueness. Aeromagnetic data have consistently been used in mineral exploration and geological mapping such as faults since the early 1960s [1,2,3,4,5]. These variations are related to changes of structures, magnetic susceptibilities and/or remnant magnetization. Sedimentary rocks, in general, have low magnetic properties compared with igneous and metamorphic lithotypes that tend to have a much greater magnetic content. Thus, most aeromagnetic surveys are useful to map structure of the basement and intruded igneous bodies from basemen complex [6,7,8,9, 10,11,12]. The interpretation of aeromagnetic maps involves interpreting the basement structures and detailed examination of structures and lithologic variations in the sedimentary section. Magnetic basement is an assemblage of rocks that underlie sedimentary basins and may also outcrop in through structural windows [13, 14]. The main purpose of the aeromagnetic survey is to detect minerals or rocks that have unusual magnetic properties which reveal themselves by causing anomalies in the intensity of the earth's magnetic field [15]. The aeromagnetic survey is applied in mapping these anomalies in the earth's magnetic field and this is correlated with the underground geological structure. Faults usually show up by abrupt changes or close spacing in orientation of the contours as revealed by the magnetic anomalies [16]. Most mineral deposits are related to some type of deformation of the lithosphere, and most theories of ore formation and concentration embody tectonic or deformational concepts [17, 18]. Some lineament patterns have been defined to be the most favourable structural conditions in control of various mineral deposits [19]. This paper presented the results of aeromagnetic interpretation for purpose the identifying of the major faults of the investigated area. The investigated area is very important in order to trace out the lineaments like faults and fractures, to delineate lithologic boundaries as revealed by magnetic disturbances caused by different rock types and to determine the depth to basement.

1.1 Site Description and Geology of the Study Area

The study area is situated in the southwestern part of the Ilesha, Osun State, Nigeria and lies within the coordinates latitude 7°32′20″ to 7°38′20″ North and longitude 4°36′20″ to 4°44′20″ East (Fig. 1). Major and minor road linkages characterize the study area linking both towns and villages in the area. The topography of the area is generally flat and punctuated in some areas by hilly ridges and gentle steeps with elevation of 320 to 390 m above sea level. The study area falls within the Guinea Savannah belt of Nigeria but exploitation and other human activities have gradually changed the vegetation to that of Sudan Savannah [20]. Geologically, the investigated area is concealed with the Southwestern Nigeria, in which the basement complex composing migmatitegness complex, metaigneous rock such as pelitic schist, quartzite, amphibolites, charnokitic rocks, older

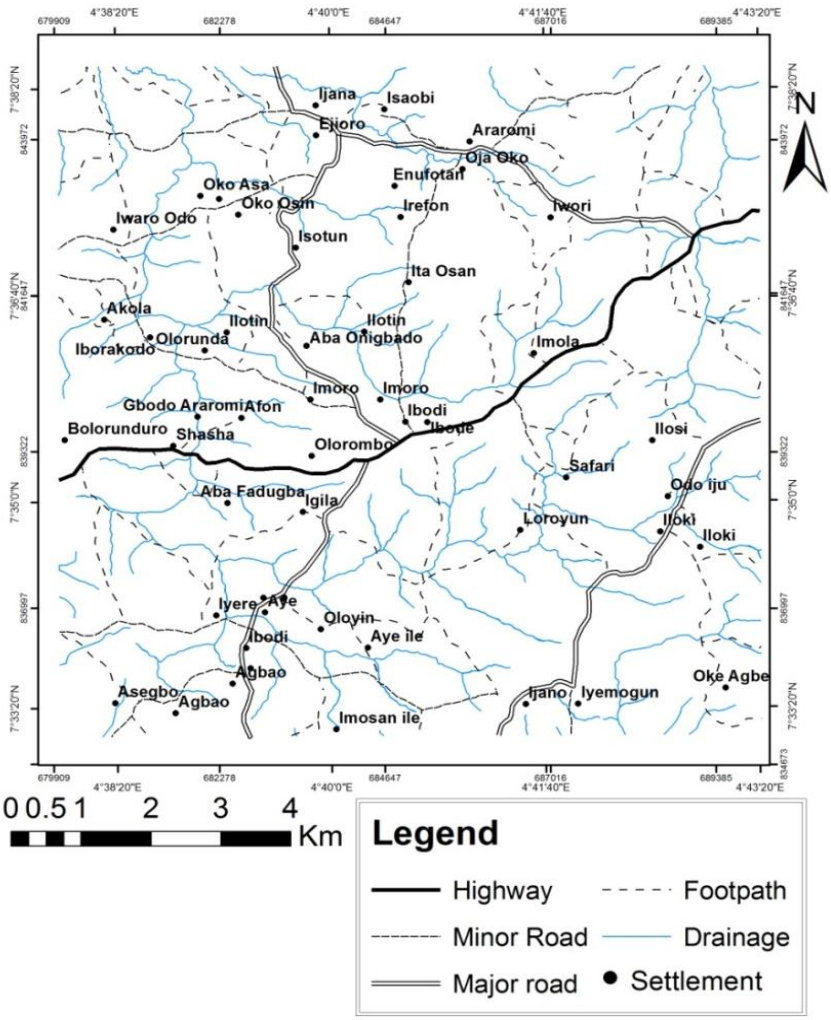

Fig. 1. Location map of the study area

granite and unmetamorphorsed dolerite dykes. The rock sequence consists of basically weathered quartzite older granite, follow by heterogeneous assemblages [21]. The geology of the investigated area is mainly Precambrian Basement rock. This is because of the tectonics and metamorphic changes that has occurred in the area [22]. The following series of rock stands out in the Precambrian Basement rock of the study area vis-à-vis amphibolites, schist and amphibolites and Gneiss and migmatite undifferentiated (Fig. 2).

2. RESEARCH METHODOLOGY

The remote sensing data (Lands at imagery) were acquired from the Global Land Cover Facility homepage and the automatic lineament extraction process was carried out using "ENVI" 4.5, "Geomatical'' pcl and "ArcGIS'' 10.2 software which was used for digital image processing and lineament extraction. An aeromagnetic map on a scale of 1:50,000 were acquired from the Nigerian Geology Survey Agency (NGSA). The aeromagnetic data was acquired at a nominal flying altitude of 152 m (about 500 ft) with flight lines spaced 2 km in the direction 60/240 (dip/azimuth) degree and contour interval of 20 nT. Magnetic instruments used are airborne magnetometers and digital data acquisition system track recovering system, recording altimeters, magnetic compensation unit and Doppler navigation system. Regional correction was based on IGRF (1st January, 1974). The processed airborne magnetic field intensity was enhanced through the removal of the International Geomagnetic Reference Field (IGRF) over the area. The data projection used is

the Universal Transverse Mercator (UTM) Geosoft Oasis Montaj™ version 6.4.2 (HJ) software was used in processing the aeromagnetic intensity data. Other software applications used include Surfer ™ Version 12 and ArcGIS version 10.5 for data analysis and integration. To enhance the quality of the data and separate anomalies of shallow sources from deep sources; filters were applied on the total magnetic intensity map in which the residual map of the study area was generated. Total horizontal derivatives of potential field data was generated involving derivation of the square root of the sum of squares of the x-and y-derivatives of the magnetic intensity data. The Euler deconvolution of the aeromagnetic field data was carried out to determine the locations and depths of the source bodies, and other geologic sources in the area, using a structural index of 0.5 and 1. The structural trends obtained from the Standard Euler Solutions from the Euler deconvolution of the aeromagnetic data were import into ArcGIS 10.5 software environment, georeferencing and digitized to generate lineament map which were used to characterize the linear features in the study area and rose diagram was generated using Georient software. Estimation of depth to magnetic sources recognized as contacts between rocks, fracture, fault and sheared zones were evaluated with the aid of spectral analysis frequency. Following the interpretation of the Landsat imagery and aeromagnetic data was used in attempt to further define the structures map delineated.

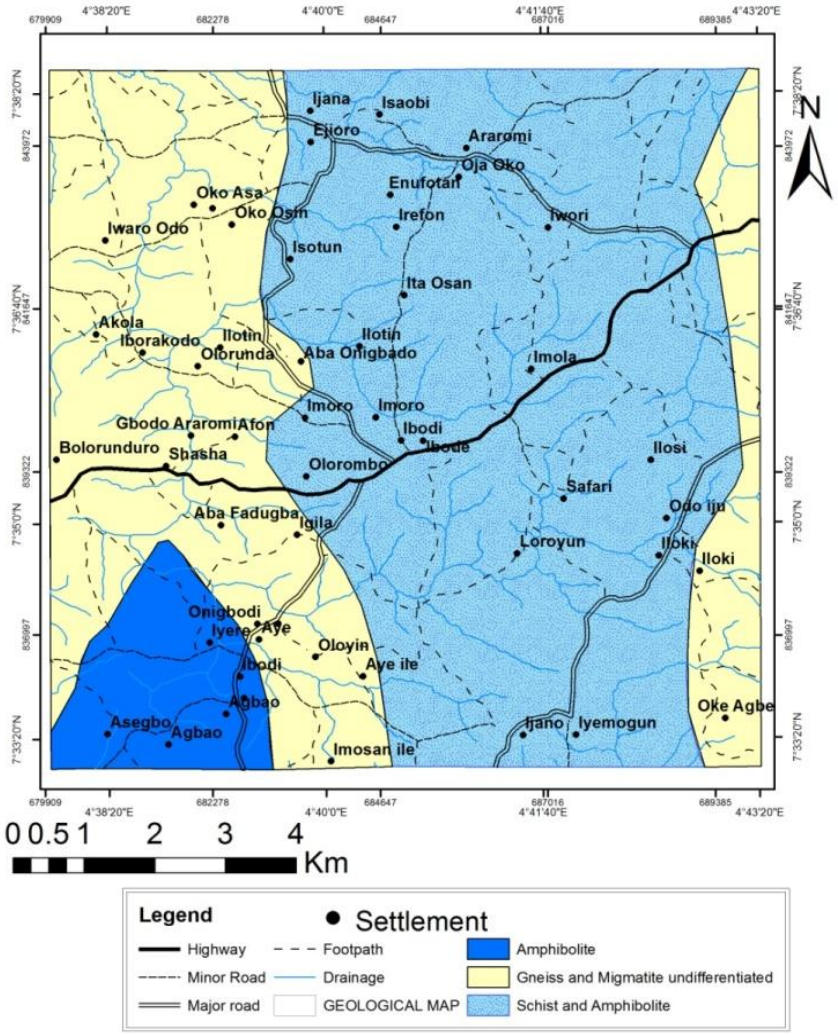

Fig. 2. Geological Map of the Study Area showing the main units as well as major regional structures

3. RESULTS AND DISCUSSION

3.1 Total Magnetic Intensity Map (TMI)

Fig. 3 illustrate the TMI image indicating high magnetic susceptible areas in low magnetic values (blue) while low magnetic susceptible areas are depicted as high magnetic values (pink colour) . Total magnetic intensity level in the study area ranges from -139.3 to 82.6 nT, suggesting contrasting magnetic susceptibilities or variation in structural extends of the rock types in the investigated area. Major positive anomalies were observed and may be attributed to the presence of gneiss and migmatite undifferentiated. Negative anomalies were observed in the area which may be due to the present of low magnetic rocks (e.g shists and amphibolites) in the area, which are noted for low magnetic signatures. The total magnetic field intensity data was gridded using the minimum curvature method. The total magnetic image showed the difference in locations of high and low magnetic intensities. The total field intensity map had earlier been corrected for large varying main earth's magnetic and temporal diurnal fields over the area.

3.2 Reduction to the Equator (RTE)

The RTE was performed to preserve low angle of inclination at the equator, thus transforming the source of magnetisation to be horizontal (Fig. 4). The output of the RTE is similar to the magnetic anomaly map of the study area because of the low angle of inclination of the area. The RTE map helps to remove magnetic inclination effect in the low magnetic latitude region by centering the peaks magnetic anomalies over their sources and enhancing the basement architecture including structural lineaments with its orientations [7]. Two major magnetic zones were identified based on the magnetic intensity variation over the study area. The Northwestern and northeastern parts are dominated by high amplitude magnetic anomalies values (between 3.7 nT and 76.6 nT). However, towards the southeastern northwestern and part of the central part of RTE, the area is characterized by relative low amplitude magnetic intensity values (between 119.3 nT and 15.5 nT) marked with greenish to blue colours suggesting regions characterized by geological structures (fracture/fault) with low magnetic contents.

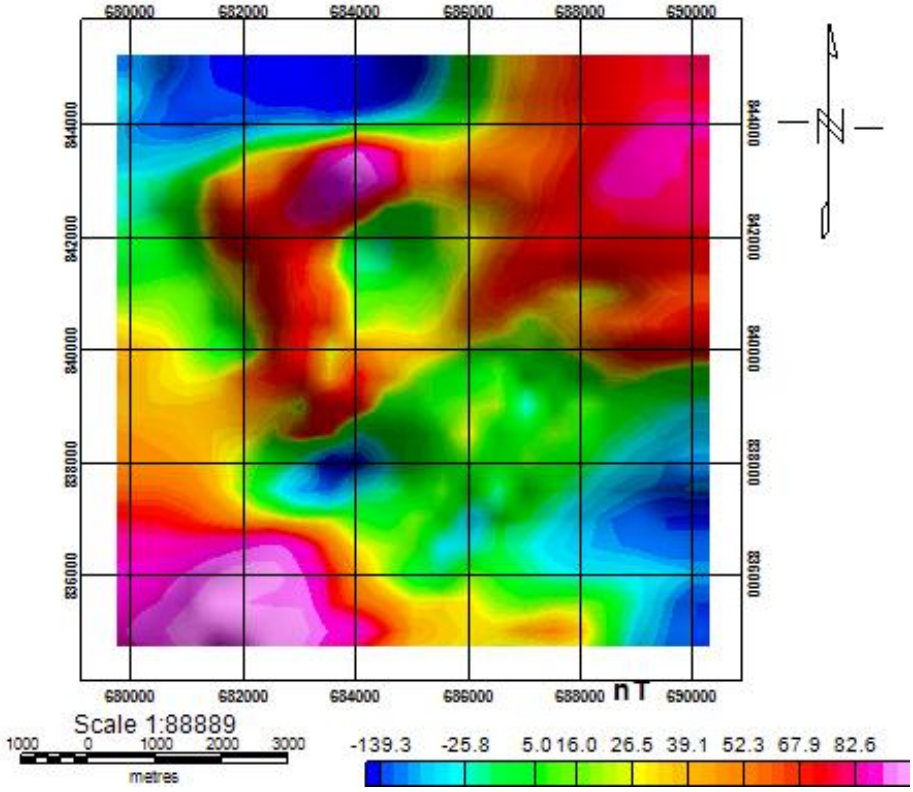

Fig. 3. Total magnetic intensity map of the study area

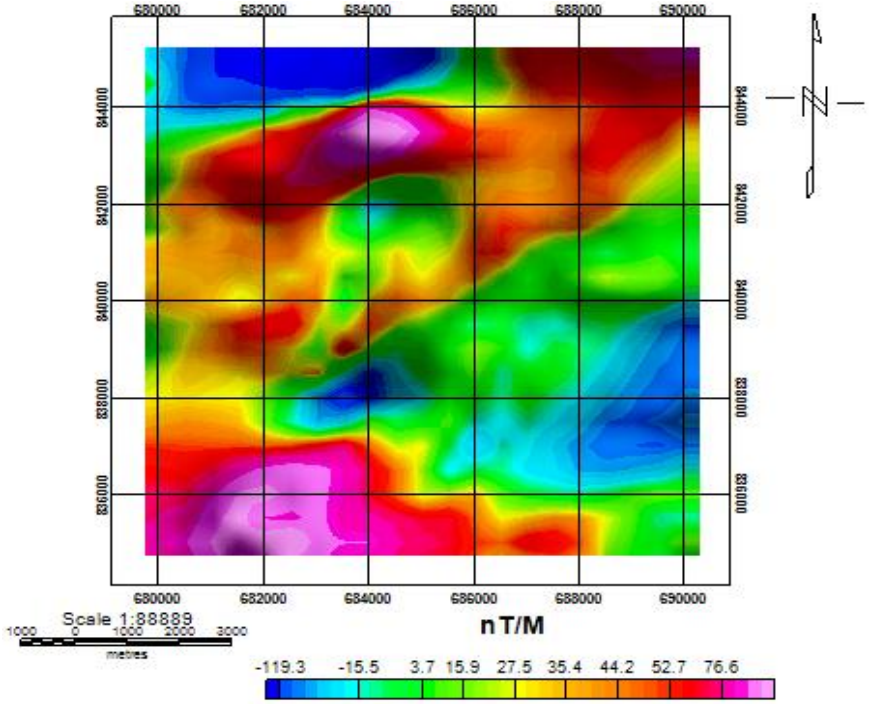

Fig. 4. Reduction to magnetic equator of the study area

3.3 Upward Continuation Map

The upward continuation of the processed TMI reduced to equator over the study area continued upward to 2 km (Fig. 5). The indentified anomaly patterns in this map are a qualitative representation of spatial variation in the magnetic properties of deep basement rocks and related structures in the area. In physical terms, as the continuation distance is increased, the effects of smaller, narrower and thinner magnetic bodies progressively disappear relative to the effects of larger magnetic bodies of considerable depth extent. As a result, upward-continuation maps give the indications of the main tectonic and crustal blocks in an area.

3.4 Residual Magnetic Anomaly Map

The Residual map obtained by removing the computed regional data (long wavelength anomalies) allows for the display of embedded residual anomalies in the original aeromagnetic map (Fig. 6). The residual magnetic anomaly map of the study area illustrated that the dominant magnetic anomaly trends in the study are predominantly in the NE-SW direction with values ranging from -104.6 to 65.8 nT. Magnetic lows were within high magnetic reliefs zones at various regions within the study area. In view of the low magnetic latitude of the study area, these magnetic lows are symptomatic of rocks with relatively higher magnetic susceptibility, a good case in point being the anomaly over the schist and amphibolites in the southwestern corner of the map.

3.5 Horizontal Derivative Map along X-Direction

Derivative filters are applied to enhance aeromagnetic signature of linear magnetic features and provides a means of enhancing anomalies of smaller and near-surface that are associated with geological structures (Fig. 7). The essence is to attenuate the long wavelength anomaly emanated from deep seated bodies and accentuate short wavelength anomaly emanated from shallow seated geologic bodies. It allows the extraction of information about the linear structures, contacts and the tectonic setting of the researched area. The color scale horizontal gradient images of the total magnetic intensity enhanced the image by showing major structural and lithological detail which was not obvious in TMI image. Geological structures were well delineated at the NE-SW direction which might be considered as the representation of fault or fracture.

3.6 Horizontal Derivative Map along Y-Direction

Derivative filters are applied to enhance aeromagnetic signature of linear magnetic features and provides a means of enhancing anomalies of smaller and near-surface that are associated with geological structures (Fig. 8). The map of the horizontal gradient in the Y direction of the study region allows the extraction of information about the linear structures, contacts and the tectonic setting. The map patterns dominated by essentially NE-SW striking anomalies are more pronounced.

3.7 Total Horizontal Derivative (THD)

Total horizontal derivative filter is an effective tool in detecting edges of magnetized structures and in the region. It tends to accentuate shallow anomalies (Fig. 9). Total horizontal derivative map was generated from the aeromagnetic data in order to enhance the anomaly curvature of the near-vertical structures arising from the changes of contrasting magnetic susceptibility. It encompasses information of the magnetic field variation along the orthogonal axes completely defining it. Consequently, structural features and boundaries of causative sources can be enhanced. Prominent structurally trend in the NW – SW and some part of northeastern directions were also in the map observed.

3.8 Analytical Signal Amplitude

The analytical signal of the magnetic anomaly field can be effectively used to map the edges of 3-D and 2-D bodies [23]. This method is based on the use of the spatial derivatives of magnetic anomalies (F(x,y)) computed along three orthogonal directions [24]. In this study, the analytical signal of the aeromagnetic data encompasses information of the magnetic field variation along the orthogonal axes completely defining it (Fig. 10). Consequently, structural features and boundaries of causative sources are determined more accurately.

3.9 Radially Average Power Spectrum

The spectral analysis of potential field data which serves as an approximate guide in estimating the depth of magnetic sources was also carried out on reduction to equator (Fig. 11). It shows a typical radial averaged spectrum of the digitized aeromagnetic data and the depth estimate plot. The theoretically average power spectrum of the study area shows a normal plot that has straight line segments which decreases in slope with increasing frequency. From the radially average power spectrum depth estimated curve, the depth to the magnetic sources in the area ranged from shallow 180 m to intermediate 280m.

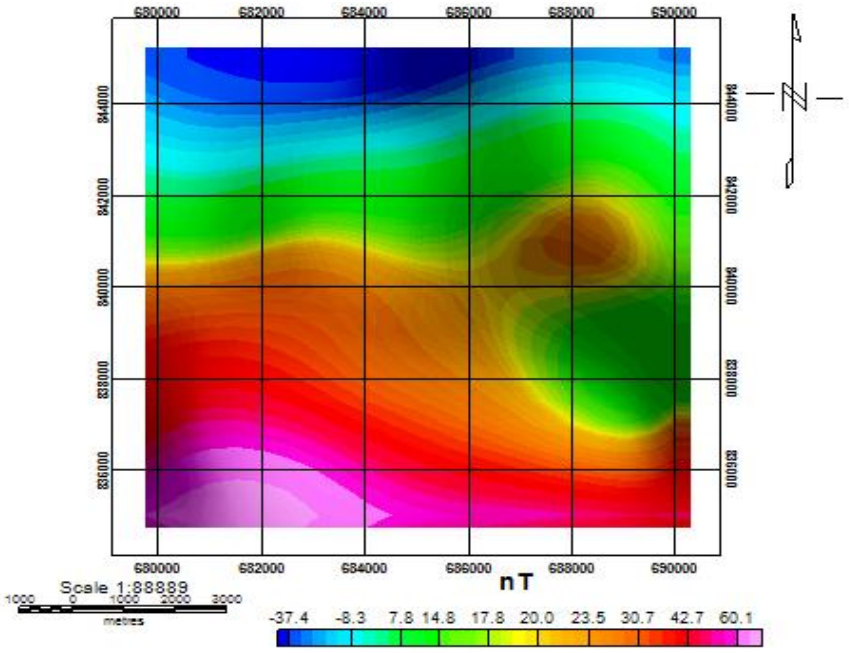

Fig. 5. Upward continuation data of the study area

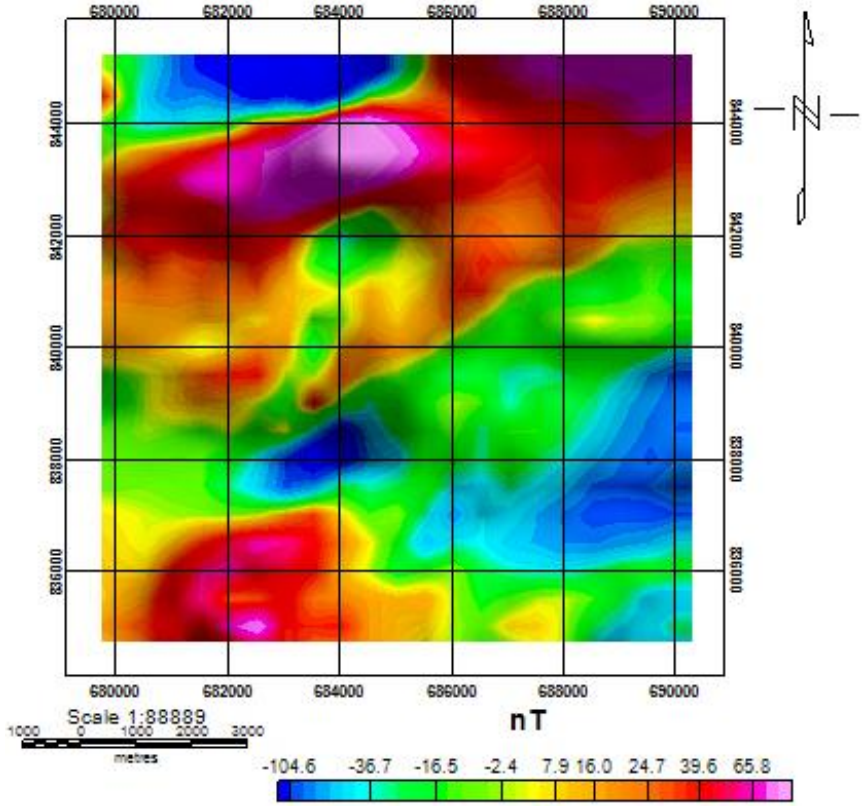

Fig. 6. Residual map of the study area

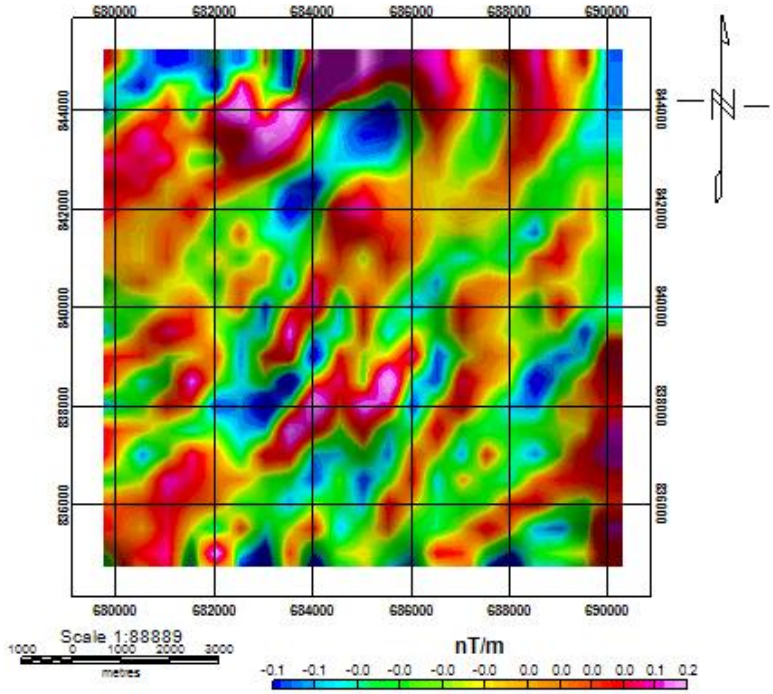

Fig. 7. Map of horizontal derivative along X-Direction

3.10 Depth Estimate Using 3D Euler Deconvolution

The Euler deconvolution of the aeromagnetic data was carried out to determine the locations and depth of the source of magnetic anomaly and other geologic sources in the area. The methodology adopted was obtaining solutions by inverting Euler homogeneity equation which relates the magnetic field and its gradient components to the location of the source of an anomaly and with the degree of homogeneity expressed as structural index. The Euler deconvolution process was carried out on the aeromagnetic data of the study area using structural index of 1.0 (Fig. 12). During the processing on Oasis Montaj software the structural index of 1.0 yielded a window size of 5 corresponding to 100 m a maximum distance of the source and a minimum depth tolerance of 15%. Depth range from 48.8 to 172.3 m was obtained, which show relatively shallow depth as related to delineated rock of boundaries. The extracted lineaments reflect the position of features such as fault, deep fractures and geologic contacts.

3.11 Aeromagnetic Lineaments Map

3D Euler solution for the aeromagnetic data of the study area, at Structural Index (S.I = 1.0) that was produced using the GEOSOFT packages was importing into ArcGIS environment. It was georeferencing and digitized to generate Aeromagnetic lineament map in Arcgis 10.5 environment with other derivatives to demonstrate the usefulness of aeromagnetic structures in lineament mapping and analysis i.e. to delineate geological structures (Fault, fracture, joint etc) in the study area. In total, 115 lineaments were extracted from the aeromagnetic structure (Fig. 13). The arose diagram prepared from the extracted lineaments on the aeromagnetic structures shows that there is one predominant sets of lineament which are closely related to tectonic activities such as fractures, faults and joints in the study area (Fig. 14). One set of the lineaments trends NE-SW directions. Major lineaments are dominated at the southeastern part whereas there are traces of minor lineament at the northeastern and central part of the study area.

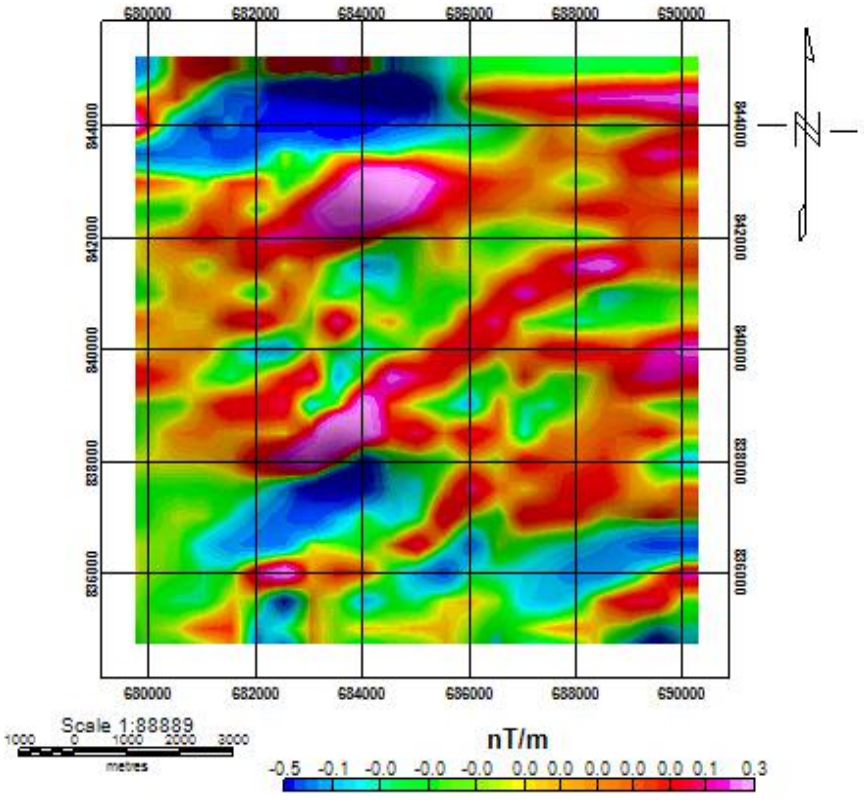

Fig. 8. Map of horizontal derivative along Y-direction

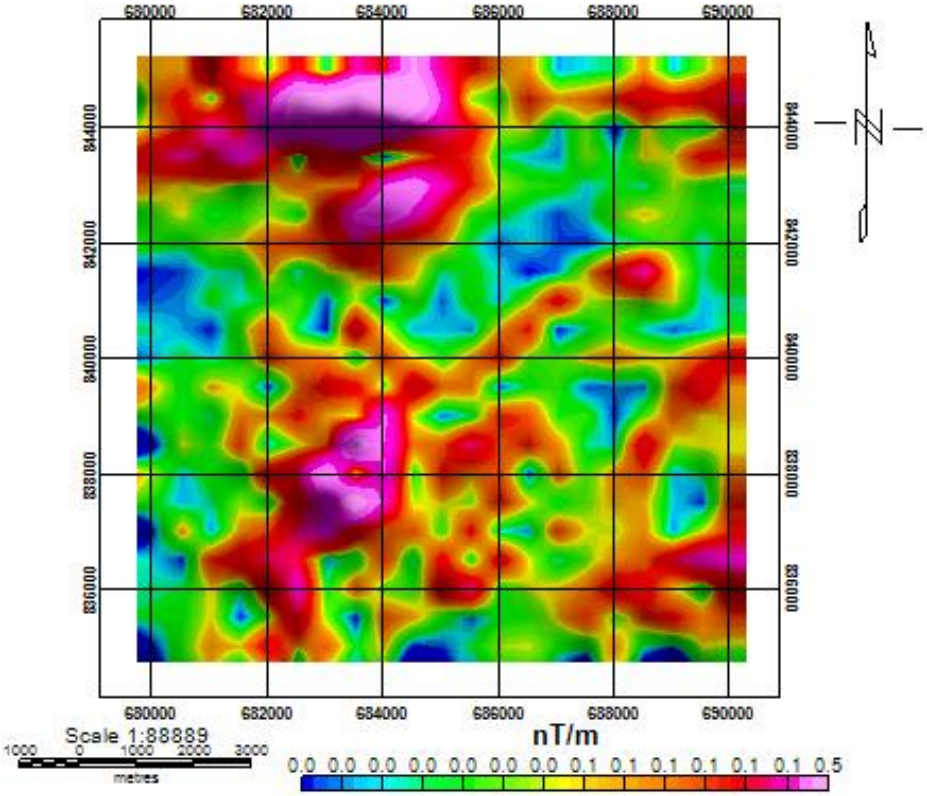

Fig. 9. Total horizontal derivative map of the study area

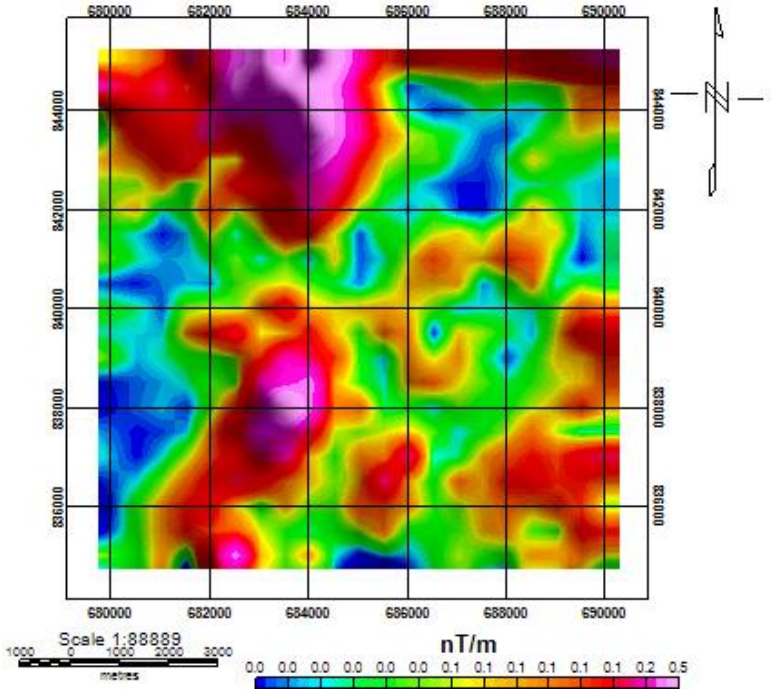

Fig. 10. Analytical signal of the study area

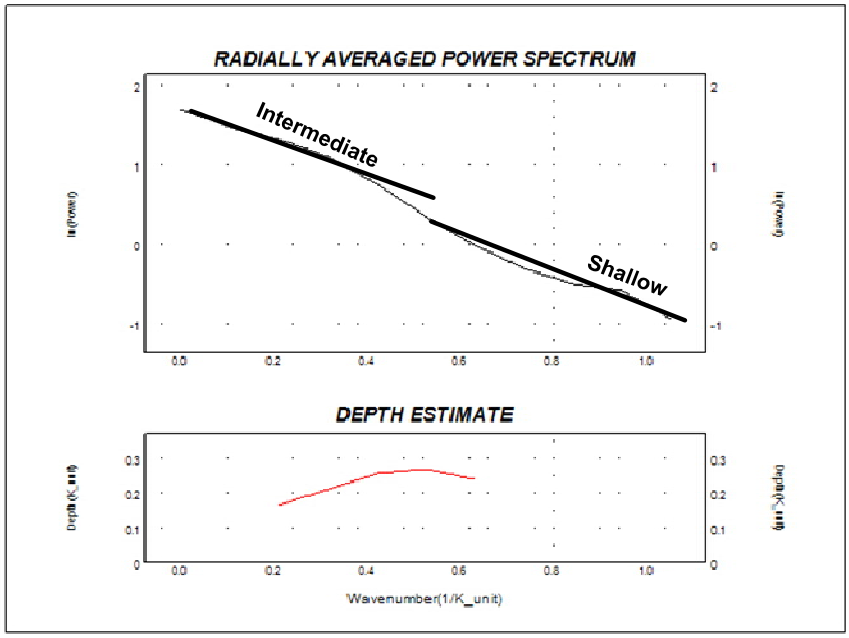

Fig. 11. Radially averaged power spectrum estimates of depth to anomaly sources

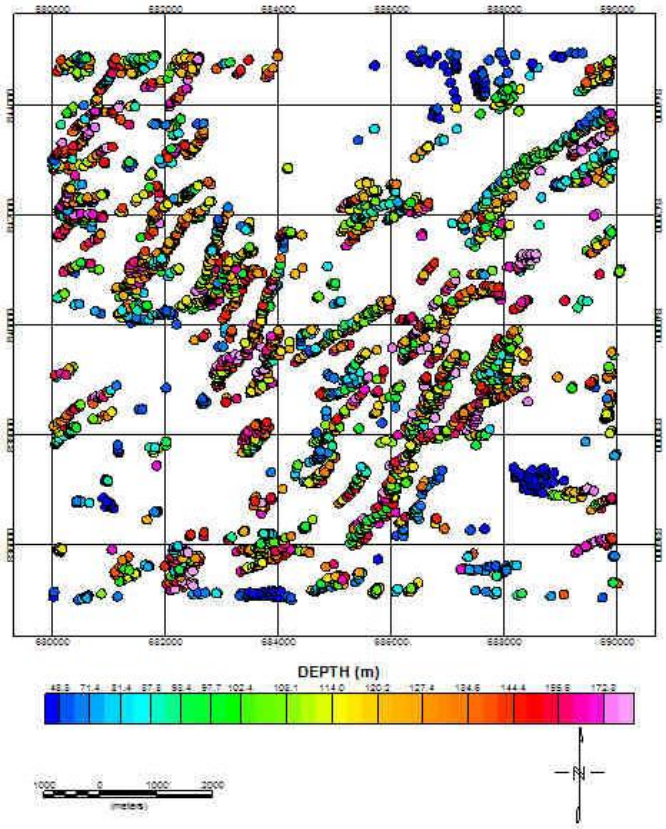

Fig. 12. Euler solution with the structural index of 1.0

3.12 Landsat Lineaments Map

Lineaments extraction was based on the identification and evaluation of the contrasting tonal effects of geomorphologic features, which are traces of fractures or fracture systems on the processed Landsat image as described by [25]. However, automated lineament extraction techniques were used in this work to increase the details of existing data of lineaments map (Fig. 15). The main advantages of automated lineament extraction over the manual lineament extraction are; the ability to uniformly approach the different images; processing operation are performed in a short time, and the ability to extract lineaments which are not recognized by human eyes. This was done by applying LINE module of PCI Geomatica 9.1 software. The map shows that the northeastern and southwestern parts are characterized by high lineaments density, while the northwestern and central parts were observed to have scanty to low lineaments density. The rose diagram of the lineaments prepared from the lineaments map shows that there was one predominant set of lineament trends which are closely related to tectonic activities resulting in features such as fractures, faults and shear zones in the study area which trends NE-SW direction (Fig. 16).

3.13 Structural Map

Integrating of the results obtained from landsat imagery, aeromagnetic structures maps and 3D euler deconvolution analysis allowed the generation of an integrated structural map of the study area (Fig. 17). This map was created from a more detailed map that showed all structures delineated by all the methods employed. It was created by using single structures (blue line) to represent all the clustered structures at an area. This was done under the assumption that the clustered structures are as a result of little discrepancies in locating the same structure by different approach. The map revealed the presence of major and minor faults, fractures as well as rock boundaries with the frequency of fracturing on different rock types. The rose diagram illustrates that most of the structures delineated are oriented in the NE-SW direction (Fig. 18). This suggests that the major fractures and faults in the study area are deep within the basement formation since the spectral analysis enhances the anomalies associated with deep magnetic sources at the expense of the dominating intermediates magnetic sources.

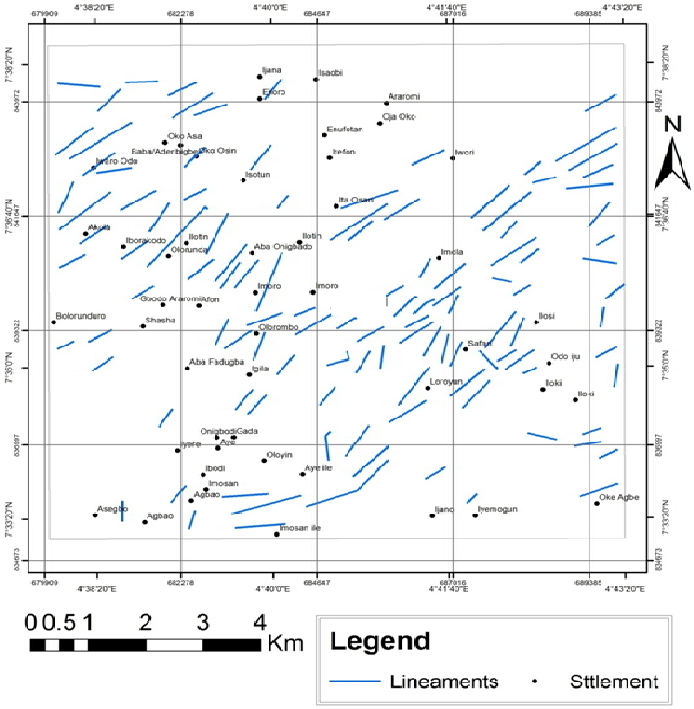

Fig. 13. Aeromagnetic lineament map of the study area

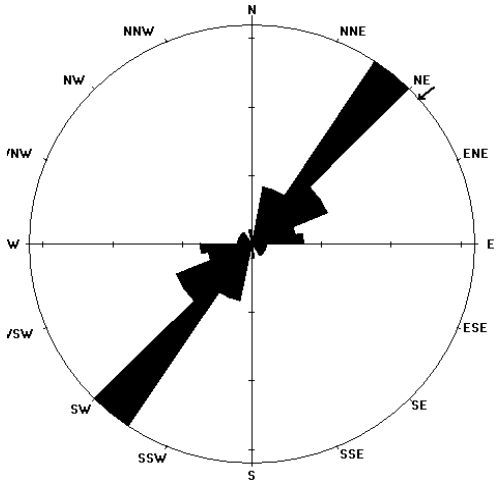

Fig. 14. Rose (Azimith-Frequency) diagram of aeromagnetic lineaments orientations landsat lineaments map

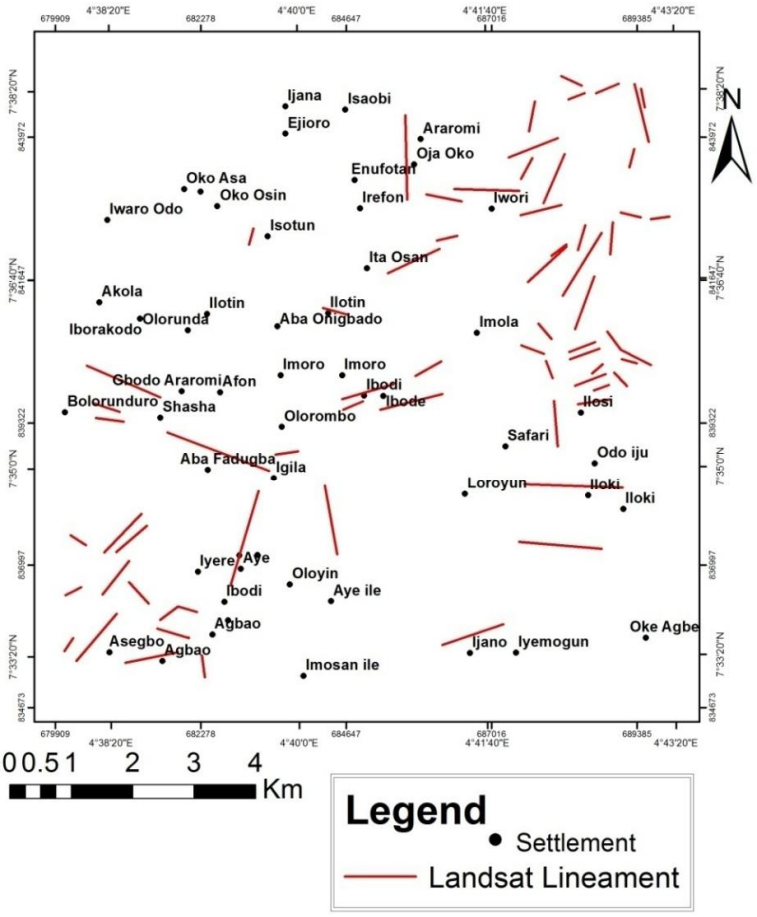

Fig. 15. Landsat lineaments map of the study area

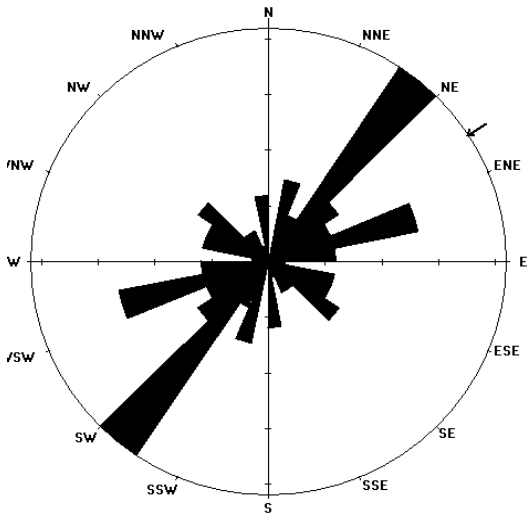

Fig. 16. Rose (Azimith-Frequency) diagram of landsat lineaments orientations

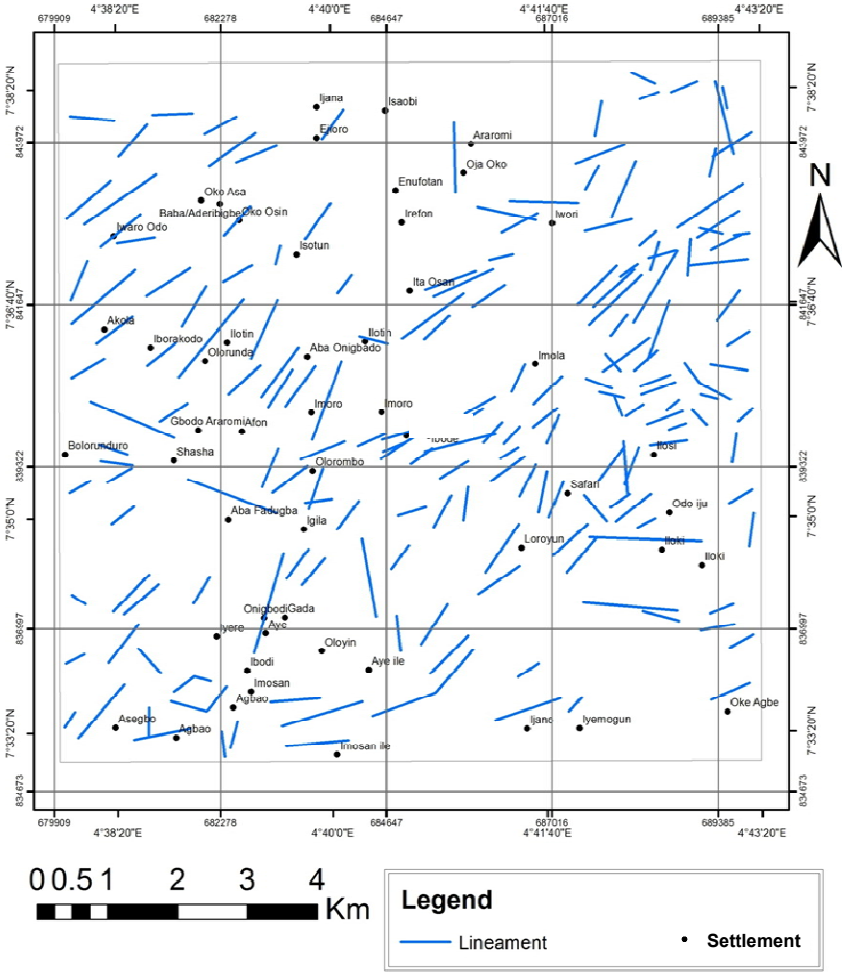

Fig. 17. Structural map of the study area

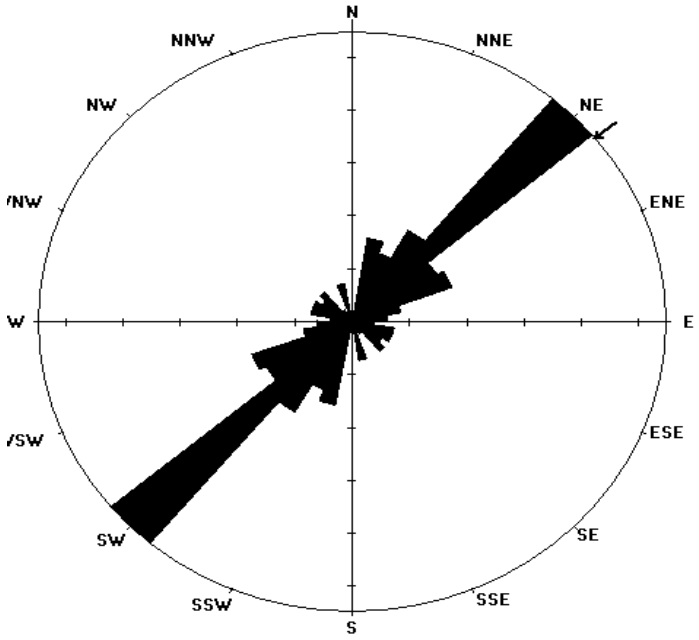

Fig. 18. Rose (Azimith-Frequency) diagram of the structural map

4. CONCLUSION

This research presents the analysis of a regional landsat imagery and aeromagnetic survey to identifying new geological structures over the investigated region. In order to map out the geological structures of the study area, magnetic image enhancing filters applied to the total magnetic intensity (TMI) using Geosoft (Oasis Montaj) are reduction to equator (RTE), total horizontal derivative (THD) and upward continuation (UC). These filters helped define the lithological boundaries, geological structures, faults, folds and contacts. The lineament of aeromagnetic map was generated from derived field intensity gradients and solutions of Euler deconvolution carried out on the aeromagnetic data using structural index of 1.0. The processed image shows the lineaments trends majorly toward NE-SW directions. These faults do not seem to be reflected in the surface but the high values of the anomalies suggest that they could have expression in depth and that they may represent important discontinuities in lithology. The 3D Euler deconvolution and radial spectral analysis applied to locate and estimate the depth to anomalous bodies, shows varying depth between 48 m and 280 m. The map revealed the presence of major and minor faults, fractures as well as rock boundaries with the frequency of fracturing. This suggests that the major fractures and faults in the study area are deep within the basement formation since the spectral analysis enhances the anomalies associated with deep magnetic sources at the expense of the dominating intermediates magnetic sources. The processed image displays the lineaments trending NE-SW directions. The new structural map derived from the interpretation of the aeromagnetic data, when combined with landsat imagery, provides an effective tool for analyzing subsurface structure in study area.

COMPETING INTERESTS

Authors have declared that no competing interests exist.

REFERENCES

1. Hood PJ. Detectability of diabase dykes by aeromagnetic surveys. Geological Survey of Canada, Report of Activities, Part B: 1967;3-9.
2. Jespersen A. Aeromagnetic interpretation of the Globe-Miami copper district, Gila and Pinal counties, Arizona. Geological Survey Research, US Geological Survey Professional Paper D. 1964;70-75.
3. Moghaddam MM, Sabseparvar M, Mirzaei S, Heydarian N. Interpretation of aeromagnetic data to locate buried faults in North of Zanjan Province, Iran. J Geophys Remote Sensing. 2015;4:143.

DOI: 10.4172/jrsg.1000143

4. Ilugbo SO, Adebiyi AD. Intersection of lineaments for groundwater prospect analysis using satellite remotely sensed and aeromagnetic dataset around Ibodi, Southwestern Nigeria. Int. J. of Phys Sci. 2017;12(23):329-353.
5. Ilugbo SO, Ozegin KO. Significances of deep seated lineament in groundwater studies around Ilesha, Southwestern Nigeria. Asian Journal of Geological Research. 2018;1(1):1-16
6. Akinlalu AA, Adelusi AO, Olayanju GM, Adiat KAN, Omosuyi GO, Anifowose AYB, Akeredolu BE. Aeromagnetic mapping of basement structures and mineralization characterisation of Ilesa Schist Belt, Southwestern Nigeria. Journal of African Earth Sciences. 2018;138:383-391.
Available:https://doi.org/10.1016/j.jafrearsci.2017.11.033
7. Olomo KO, Olayanju GM, Adiat KAN, Akinlalu AA. Integrated approach involving aeromagnetic and landsat for delineating structures and its implication on mineralization. International Journal of Scientific & Technology Research. 2018; 7(2):208-217.
8. Essam A, Ahmed S, Keisuke U. Interpretation of geomagnetic data of gabel elzeit`1 area, gulf of Suez, Egypt using magnetic Gradient Techniques. Memoirs of the Faculty of Engineering, Kyushu University. 2003;63(3).
9. Vitalis CO, Charles OO, Victor M, Gideon OL. Source depth determination from aeromagnetic data of Ilesha, Southwest Nigeria, Using the Peters' Half Slope Method, Earth Science Research. 2014; 3(1):41-47.
Available:http://dx.doi.org/10.5539/esr.v3n1p41
10. Adelusi AO, Kayode JS, Akinlalu AA. Interpretation of aeromagnetic and electrical resistivity mapping around Iwaraja area, Southwestern Nigeria. J. Geol. Min. Res. 2013;5(2):38-57.
11. Anifowose AYB, Adetunji A. Lineament studies of rocks in Omifunfun area, southwestern, Nigeria: Remote sensing and petrologic observations. Glob. J. Geol. Sci. 2015;13:1-7.
12. Akinlalu AA, Adelusi AO, Mamukuyomi EA, Akeredolu BE. Ground magneticand 2-D resistivity mapping of basement structures around Iwaraja area southwestern Nigeria. J. Basic Appl. Res. Int. 2016;18(4):206-221.
13. Onyedim GC, Awoyemi MO, Ariyibi EA, Arubayi JB. Aeromagnetic imaging of the basement morphology in part of the Middle Benue Trough, Nigeria. Journal of Mining and Geology. 2007;42(2):157-163.
Available:http://dx.doi.org/10.4314/jmg.v42i2.18856
14. John UM, Emmanuel EU. Structural analysis using aeromagnetic data: Case study of parts of southern Bida Basin, Nigeria and the Surrounding Basement Rocks, Earth Science Research. 2014; 3(2):27-42.
Available:http://dx.doi.org/10.5539/esr.v3n2p27
15. United States Geological Survey (USGS). Introduction to Potential Fields: Magnetics; 1997
16. Onuba LN, Anudu GK, Chiaghanam OI, Anakwuba EK. Evaluation of aeromagnetic anomalies over Okigwe area, southeastern Nigeria, Research Journal of Environmental and Earth Sciences. 2011;3(5):498-507.
17. O'leary DW, Friedman JD, Pohn HA. Lineament, linear, lineation: Some proposed new standards for old terms. Geological Society of America; 1976.
18. Ananaba SE, Ajakaiye DE. Evidence of tectonic control of mineralization in Nigeria from lineament density analysis A Landsat-study. International Journal of Remote Sensing. 1987;8(10):1445-1453.
Available:http://dx.doi.org/10.1080/01431168708954788
19. Megwara JU, Udensi EE. Lineaments study using aeromagnetic data over parts of southern Bida basin, Nigeria and the surrounding basement rocks. International Journal of Basic and Applied Sciences. 2013;2(1):115-124.
20. Oladejo OP, Sunmonu LA, Adagunodo TA. Groundwater prospect in a typical precambrian basement complex using Karous-Hjelt and fraser filtering techniques. J. Ind. Eng. Res. 2015;1(4): 40-49.
21. Rahaman MA. Review of the basement of S.W. NigeriaInc. Kogbe (ed) Geology of Nigeria. Elizabethan press, Lagos. 1976; 41–58.
22. Olade MA. General features of a Precambrian iron deposit and its environment at Itakpe Ridge Okene,

Nigeria. Trans. Inst. Min. Metallurgy. Sect. B. 1978;87:81-89
23. Roest WR, Verhoef J, Pilkington M. Magnetic interpretation using 3-D analytical signal. Geophysics. 1992;57(1):116-125. DOI: 10.1190/1.1443174.
24. Lanza R, Meloni A. The earth's magnetism—An introduction for geologists. Springer Verlag, Berlin, Heidelberg; 2006.
25. Ogunmola JK, Ayolabi EA, Olobaniyi SB. Lineament extraction from Spot 5 and Nigeria Sat-X imagery of the Upper Benue Trough, Nigeriaǁ, International Archives of the Photogrammetry, Remote Sensing and Spatial Information Sciences, Volume XL-1, ISPRS Technical Commission I Symposium, Denver, Colorado, USA. 2014;323-330.

Peer-review history:
The peer review history for this paper can be accessed here:
http://www.sdiarticle4.com/review-history/57292